

# Analysis Of Transformer Bias Vibration Based On "magnetic-mechanical" Coupling

Junqiang Xing\*, Zhuwen Dai, Wendi Yu, and Yunshuo Zhang

School of Electrical Engineering, Shenyang Institute of Engineering, Shenyang, Liaoning, 110136, China

\* Corresponding author. E-mail: xingjq@sie.edu.cn

Received: Feb. 23, 2023; Accepted: Jun. 26, 2023

---

The large-scale application of flexible DC power transmission technology leads to DC bias in transformer cores, and the vibration analysis of transformers under the influence of DC bias is becoming a hot topic. In this paper, based on the "electromagnetic-mechanical" coupling model, we propose a bias vibration analysis method for large power transformers. The electromagnetic forces calculated in the electromagnetic field are mapped to the surfaces of structural members and tanks in the structural force field by means of a grid mapping method, facilitating the direct calculation of transformer vibration displacements under DC bias conditions. Finally, based on the coupled magnetic-structural analysis, the maximum deformation of different structures of the transformer under different DC bias magnetism is studied. The vibration response band of the transformer is above 100Hz, where the DC input of 25A per phase causes the maximum displacement deformation of 39.06mm in the transformer tank, which provides the analysis basis for the safe operation of the transformer.

**Keywords:** transformer, vibration, DC bias, magnetic, mechanical

© The Author(s). This is an open-access article distributed under the terms of the [Creative Commons Attribution License \(CC BY 4.0\)](https://creativecommons.org/licenses/by/4.0/), which permits unrestricted use, distribution, and reproduction in any medium, provided the original author and source are cited.

[http://dx.doi.org/10.6180/jase.202404\\_27\(4\).0014](http://dx.doi.org/10.6180/jase.202404_27(4).0014)

---

## 1. Introduction

With the wide application of high-voltage DC transmission system, it will make the transformer neutral point DC bias magnetization phenomenon, DC bias magnetization will lead to abnormal transformer vibration, noise intensification, long-term under the influence of bias magnetism will occur in the transformer winding deformation, loosening and other fault probability increased, affecting the stable operation of the transformer [1]. Therefore, it is necessary to study and analyze the vibration characteristics under DC bias magnetism. The vibration source of transformers mainly comes from the core and winding, and long-term operation will lead to vibration on the surface of the tank [2]. However, the core vibration will directly lead to the vibration and deformation of the pulling plate and clamped parts. Therefore, this paper will focus on the vibration displacement of the structural parts and tank of the trans-

former under different DC bias magnetism by combining the transformer core, pulling plate and clamped parts as the research object [3].

At present, the study of transformer performance from vibration analysis, its research process can be divided into two directions, one is the study of transformer vibration mechanism, Peiyu Jiang et al. measured the hysteresis expansion and contraction characteristics of oriented silicon steel sheet in the condition of with and without DC bias magnetization, measured the core vibration with laser vibrometer, and established a model to verify the effectiveness of frequency domain decomposition algorithm [4]; Xingmou Liu et al. introduced DC excitation at the neutral point and measured the transformer excitation and vibration characteristics and proved that DC bias magnetization has a large influence on the direction and symmetry of magnetostriction [5]; Second, the study of transformer vibration monitoring. Shuhan Jin et al. analyzed the three-

phase three-column transformer noise data based on the abnormal noise data, and concluded that the transformer noise is caused by the small DC current flowing about 1A through the neutral point of the transformer by testing and spectral analysis [6]; Zhendong Zhang et al. used a single-phase three-column transformer for no-load and partial-load DC bias tests to measure the time domain waveforms of transformer excitation current and vibration noise and their spectral distributions to provide a reference for DC bias tolerance under actual operating conditions [7]. Most of the current researchers directly study the transformer vibration under different DC bias based on transformer models or actual transformers [8–10], without linking the changes of transformer excitation state under DC bias with the vibration characteristics. The method proposed in this paper is based on the magnetic-mechanical coupled field theory to calculate the bias magnetic vibration of transformers, which can not only accurately reflect the frequency and energy change of the vibration signal with time, but also realize the simulation analysis of the whole process of the vibration response of the core excited by electromagnetic force during the operation of transformers.

## 2. Mathematical model of transformer magnetic field coupling

If a DC current  $i_{dG}$  is passed into the secondary winding of a single-phase transformer, which produces a DC bias flux of  $\Phi_0$ , the total closed flux of the core is:  $\Phi = \Phi_0 + \Phi_m$ . Let the average length of the core's magnetic circuit be  $l$ . According to Ampere's law of loops, the equation of magnetic potential balance can be obtained as [11].

$$N(i_{ac} + i_{dc}) = Hl \quad (1)$$

A bias electromagnetic field will be formed when a bias current is passed through the transformer winding. Establishing a mathematical model of the magnetic field force of the core is the basis for studying the vibration of the core, and it is known from the full current law that the magnetic field strength at DC bias magnetization is

$$H = \frac{Ni}{l} = \frac{N(i_{ac} + i_{dc})}{l} = H_{ac} + H_{dc} \quad (2)$$

which:  $H$  is the magnetic field strength,  $i$  is the current rms value,  $l$  is the main magnetic circuit length,  $N$  is the number of turns of the coil,  $i_{ac}$ ,  $i_{dc}$  are the AC and DC current rms values,  $H_{ac}$ ,  $H_{dc}$  are the AC and DC magnetic field strengths, respectively.

To obtain the analytical expression of the electromagnetic force on the core, the excitation model of the transformer is simplified and the magnetic field volume force

density of the linear, isotropic ferromagnetic material is obtained based on the electromagnetic field theory.

$$f = J \times B - \frac{1}{2} H^2 \nabla^2 \mu + \frac{1}{2} \left( H^2 \tau \frac{\partial \mu}{\partial \tau} \right) \quad (3)$$

where  $f$  is the magnetic force bulk force density,  $J$  is the circuit density vector,  $B$  magnetic induction intensity vector,  $H$  is the magnetic field strength,  $\mu$  is the magnetic permeability of the material and the material, and  $\tau$  is the bulk density. In addition, the first term in Eq. characterizes the Lorentz force, the second term characterizes the material bulk force, and the third term characterizes the magnetostriction.

The magnetic field can be divided into  $x$ ,  $y$  and  $z$  directions in the silicon steel sheet and the expressions for each of the three directions are listed according to Eq. (3). For the convenience of analysis in this paper, the deformation in the  $z$ -direction is the main feature of the deformation of the silicon steel sheet in the excitation state, so the bulk force density in the  $z$ -direction in Eq. (2) is written as

$$f_z = \frac{\partial}{\partial z} \left[ \mu H_z^2 - \frac{H^2}{2} \left( \mu - \tau \frac{\partial \mu}{\partial \tau} \right) \right] + \frac{\partial}{\partial x} (\mu H_x H_z) + \frac{\partial}{\partial y} (\mu H_y H_z) \quad (4)$$

Neglecting the local leakage, the magnetic flux can be considered to be concentrated in the magnetic circuit of the core. Taking into account the symmetry of the core structure, the  $x$  and  $y$  coordinate planes are chosen as the symmetry planes. If the direction of  $x$ -axis is parallel to the direction of magnetic field, there is

$$H = H_x(y, z), H_y = H_z = 0 \quad (5)$$

Substituting Eq. (5) into Eq. (4), obtain Eq. (6)

$$f_z = \frac{\partial}{\partial z} \left[ -\frac{H^2}{2} \left( \mu - \tau \frac{\partial \mu}{\partial \tau} \right) \right] \quad (6)$$

Then the magnetic field force  $F$  in the  $z$ -direction can be expressed as

$$F = \int_V f_z dV = k \int_V f_z dV = k \frac{\partial}{\partial z} \left[ -\frac{H^2}{2} \left( \mu - \frac{\partial \mu}{\partial \tau} \right) \right] dx dy dz \quad (7)$$

Where  $k$  is the curvature of its middle surface in the  $x$  and  $y$  directions after bending the silicon steel sheet.

## 3. Modeling of the transformer

### 3.1. Finite element modeling of transformer

The magnetic simulation is mainly to solve the MagNet equation system by the finite element method to get the

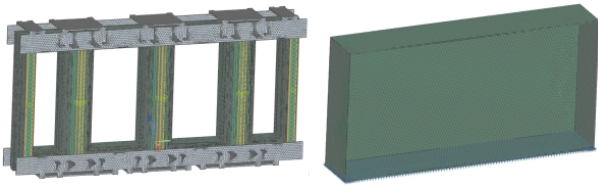


**Fig. 1.** Transformer structural parts geometry model

distribution and size of the required parameters such as magnetic flux density, electromagnetic force and current density [12]. Large experiments have been conducted to prove that the vibration of the core in the no-load condition is larger than that of the winding in the short-circuit condition, so this paper takes the no-load condition as the analysis condition, when the vibration displacement is mainly generated by the core hysteresis. The simulation calculation of electromagnetic field and electromagnetic vibration is realized by MagNet, and the simulation calculation of vibration displacement is realized by Simcenter 3D. The model material settings for the application transformer core and oil tank are shown in Table 1.

A three-phase, five-column transformer with a capacity of 420 MVA and a voltage level of 354 kV is used to calculate the inherent frequency and modal vibration pattern of the structural components. Considering the small mass of the clamping and fixing parts compared to the transformer core, the clamping parts can be omitted in the process of vibration analysis of the transformer after setting the corresponding preload on the contact surface of the clamping parts and the silicon steel sheet to simplify the calculation model. Therefore, the geometric model of the simplified 3D solid structural parts of the power transformer is shown in Fig. 1.

Under the action of a magnetic field, the ferromagnetic material forming the core of a transformer undergoes a dimensional change called the magnetostriction effect. Magnetostriction is one of the main causes of transformer core vibration [5]. Therefore, in this paper, we only study the effect of the paramagnetic vibration of structural components driven by the hysteresis characteristics of the core, and the effect on the end winding and insulation structure is not analyzed for the time being. Due to the symmetry of the transformer model, the oil tank is simplified to one-half model for calculation. In addition, geometric boundary conditions need to be imposed on the simulation model, i.e., the core-structural member and the bottom of the tank are fixed constraints.

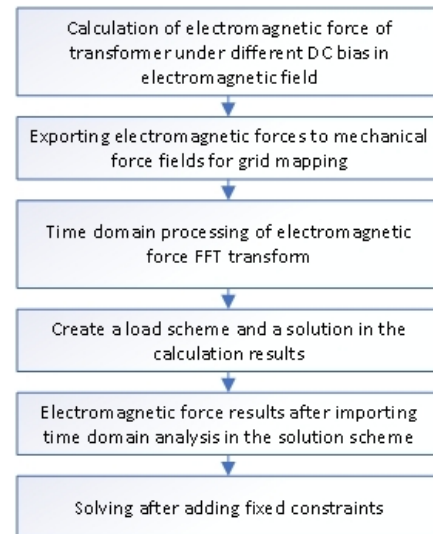


**Fig. 2.** Calculation steps of transformer bias vibration

### 3.2. Electromagnetic force-mapping loading

The main calculation flow of transformer vibration response under different DC bias magnetism is shown in Fig. 2, where the mapping of electromagnetic forces loaded onto the structural grid of the transformer core and tank is an important part of the transformer bias vibration calculation.

Since the vibration analysis is performed in the frequency domain, a harmonic response analysis is required in order to calculate the electromagnetic force node distribution conditions of the transformer core, tie plate and clamp members and other structural components. Firstly, the transformer finite element model was loaded with off-street electromagnetic force load by using the electromagnetic simulation and analysis software Magnet. Then, the electromagnetic force load file obtained from the analysis is imported into the Nastran solver in Simcenter 3D, and the excitation force loading of the structural finite element model can be realized. Due to the consistent distribution of mechanical mesh and structural mesh nodes, the electromagnetic force can be accurately mapped to the surface of the core and oil tank. The mesh mapping of transformer structural parts is shown in Fig. 3.

Based on the calculated electromagnetic force magnitude and point distribution of each transformer component in the electromagnetic field, the output electromagnetic force is a time-domain value, and it is necessary to import the electromagnetic force data into the FFT module for transformation to obtain the amplitude and phase angle of the main harmonics after DC bias magnetization before mapping. The corresponding frequency amplitudes and

**Table 1.** Material properties of transformer components

Parts	Materials	Density kg/m <sup>3</sup>	Elastic modulus pa	Poisson ratio
core	27ZH095	7650	$2 \times 10^{11}$	0.3
tank	Carbon steel Q345b	7850	$2 \times 10^{11}$	0.3

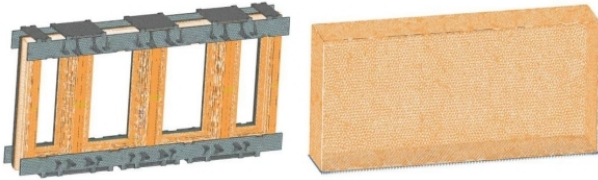


**Fig. 3.** Mesh mapping of transformer structural components

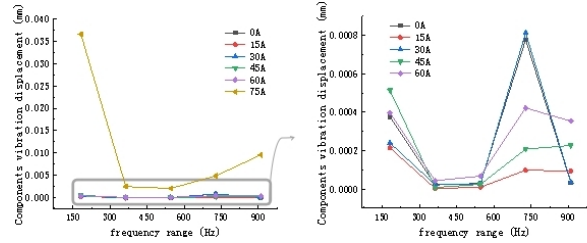


**Fig. 4.** Vibration displacement of a structural member under DC bias magnetism

phase angles are applied equally to each node on the surface of the structure and tank, thus forming a closed loop for coupled iterative calculations. As an example, the amplitude of the main harmonics of the transformer in the DC bias condition is shown in Table 2 for a DC input of 20 A per phase at the neutral point of the transformer.

**4. Transformer vibration displacement calculation analysis**

**4.1. Vibration calculation of core-structure parts**

In order to find out the electromagnetic force distribution of the transformer under different DC bias conditions, it is necessary to input DC currents of 0A, 15A, 30A, 45A, 60A and 75A into the neutral point of the transformer in the electromagnetic field in turn, and it is solved that DC 75A is the maximum DC current that this transformer can withstand. In the vibration analysis, ignoring the electromagnetic component force of small amplitude, the FFT transform results of the dominant component force are shown in Fig. 4. According to the experimental results, it is found that the electromagnetic forces under different DC bias magnetization are transformed by FFT to obtain the displacements at five different frequencies, which are 181.82Hz, 363.64Hz, 545.45Hz, 727.27Hz and 909.09Hz, thus proving that the vibration signal frequency of the transformer under the action of DC bias magnetization contains not only the even harmonic components, but also the odd harmonic components rising in different degrees.

The main response band of this core-structure member is above 100Hz, and the amplitude spectrum energy is mainly concentrated around 200Hz, 700Hz, and the vibration displacement tends to become larger as the DC current increases, although the amplitude at the main vibration fre-

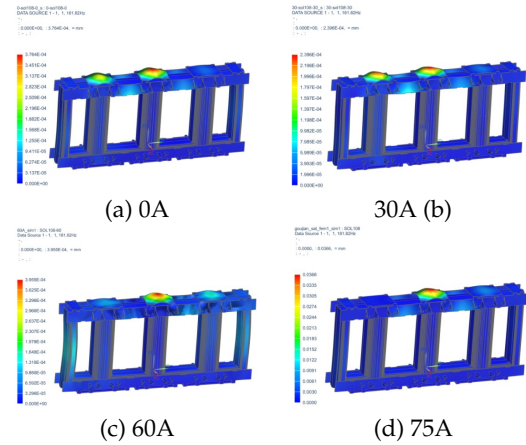


**Fig. 5.** Vibration displacement of structural parts at 200Hz under different DC bias magnetism

quency fluctuates within the normal electromagnetic force range, but the fluctuation is small, about 8.13E-04mm. Based on the values of vibration displacement at each frequency under different DC bias magnetism, a polynomial curve can be fitted, and the vibration displacement versus frequency can be expressed by Eq. (8), where  $f$  represents the frequency and  $D$  represents the vibration displacement.

$$D(x) = -1.507e - 11 \times f^3 + 2.563e - 08 \times f^2 - 1.279e - 05 \times f + 0.001935 \tag{8}$$

According to the relevant research data, the transformer vibration frequency under normal condition is within 600Hz, so this paper only analyzes the transformer vibration displacement at 200Hz and 550Hz, and the maximum amplitude is up to 5.71E-04mm. As shown in Fig. 5.

**Table 2.** Transformer electromotive force at 60A DC for each harmonic

Frequency (Hz)	Von-Mises (N/m <sup>2</sup> ) (Isoelectric force)	Average stress (N/m <sup>2</sup> )	Maximum principal stress (N <sup>2</sup> /m <sup>2</sup> )	Minimum principal stress (N/m <sup>2</sup> )
181.82	0.0426	0.0276	0.0528	0.0139
363.64	0.0225	0.01033	0.0234	0.002542
545.45	0.0225	0.0103	0.0234	0.00379
727.27	0.0921	0.0552	0.1166	0.025
909.09	0.0956	0.0668	0.0387	0.1172

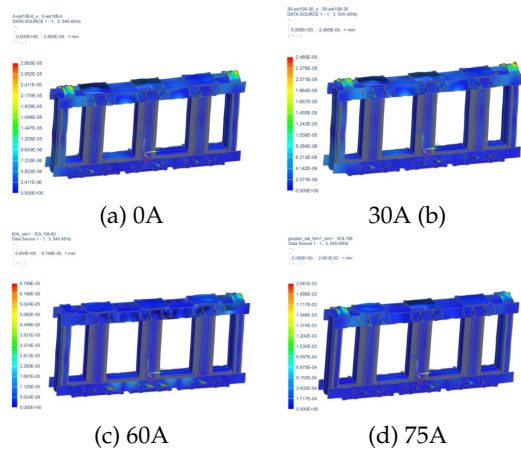


**Fig. 6.** Vibration displacement of structural parts at 500Hz under different DC bias magnetism

Under the different DC bias , the vibration displacement of the transformer structure at 200 Hz, the deformation is mainly located in the core column at the clamped parts, and the corresponding clamped parts deformation in the B-phase core column is larger than the corresponding clamped parts deformation in A and C. This is due to the magnetic flux concentration in the core column, and the magnetic induction intensity in the middle is larger than the magnetic induction intensity at both ends. The larger stress in the core is mainly distributed at the connection between the core column and the yoke. As the input DC current increases, a certain degree of deformation occurs in the center of the transformer core side column.

As shown in Fig. 6, the deformation of the vibration displacement of the transformer structural parts at 500 Hz is mainly located in the middle of the upper clamped parts of the transformer and the left and right sides of the lower clamped parts surface, and the displacement caused by the deformation is fluctuating, and the maximum range of displacement reaches about 2μm. Asymmetry appears at the left and right ends of the clamp, indicating that the deformation of the upper surface of the core exerts a force on the clamp.

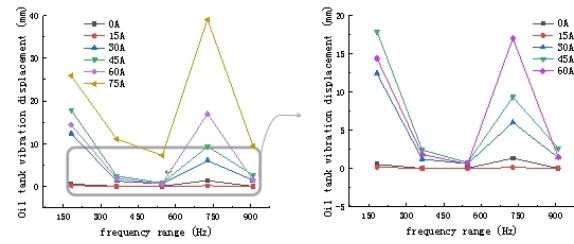


**Fig. 7.** Vibration displacement of tank under bias magnetic condition

**4.2. Vibration calculation of fuel tank**

The results of the core-structure vibration displacement of the transformer show that the autotransformer mainly exhibits vibration at 200Hz under no-load condition. Input different DC currents, the vibration displacement curve of the transformer tank can be seen from Fig. 7.

The main response frequency band of this tank is above 100Hz, the amplitude spectrum energy is mainly concentrated in the vicinity of 200, 700Hz, and the structural parts of the amplitude spectrum of deformation of the same range, from the value of the maximum deformation of 39.06mm, at the moment of 25A DC per phase for the transformer core is saturated; in the neutral point Input DC 30A transformer tank deformation began to change abruptly, and with the increase of input DC current, the transformer tank by the electromagnetic force caused by the deformation displacement also gradually increased, in the normal electromagnetic force range, its main vibration frequency fluctuations are small, about 1.352mm. Likewise, polynomial curve fitting of each bias vibration data of the tank yields the fitting equation, i.e., the relationship between tank vibration displacement and frequency expressed in Eq. (9), which plays an active role in controlling the stable operation of the transformer when subjected to bias magnetism.

$$D = -2.674e - 07 \times f^3 + 0.4629e - 03f^2 - 0.2418f + 39.63 \tag{9}$$

As shown in Fig. 8, the deformation of the transformer tank under DC bias at 200Hz mainly occurs at the cover and

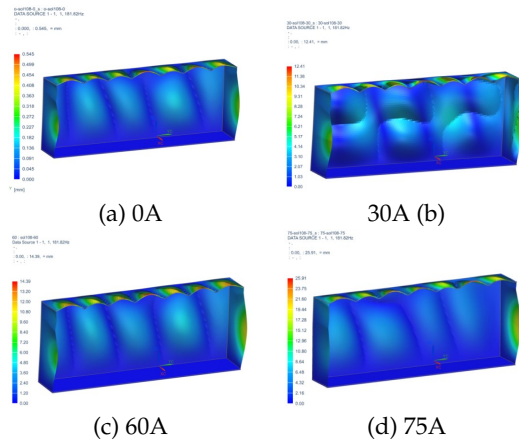


**Fig. 8.** Vibration displacement of tank at 200Hz under different DC bias magnetism

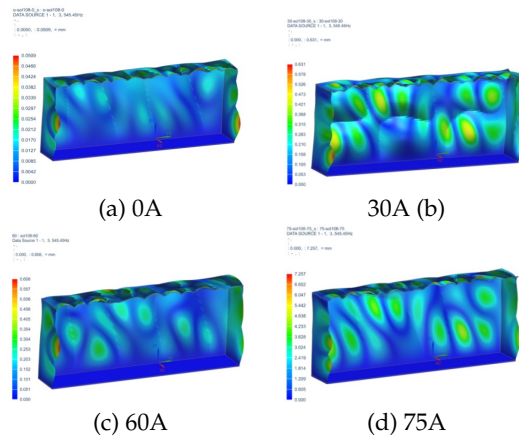


**Fig. 9.** Vibration displacement of tank at 550Hz under different DC bias magnetism

box, the deformation of its cover is larger, the maximum deformation is the vibration displacement of 25.91mm at DC 75A, the box wall also has different degrees of vibration deformation, which A, B, C three phase core vibration signal are transmitted to the transformer tank with transformer oil as the medium, causing the surface of the transformer tank vibration.

In the case of frequency of 550Hz, as shown in Fig.9, in the frequency of vibration deformation mainly occurs in the box surface of the middle of the upper position, the vibration displacement of the maximum value of 7.25mm, which is due to the lower part of the transformer body fixed constraints, so the vibration generated by the core from the bottom up to the heart column - upper yoke - tank cover in order to conduct.

## 5. Conclusion

1. This paper analyzes the vibration characteristics of transformer core-structure parts and oil tank under different bias magnetism for a three-phase five-column transformer transformer DC bias magnetism vibration, which shows that the main response band of transformer bias magnetism vibration is above 100Hz, and is affected by DC bias, due to the transient components contained in the excitation current, the transformer components contain both even and odd frequency components in their vibrations, of which the maximum vibration displacement occurs near 200Hz, with displacement  $5.71E-04$ mm.
2. Secondly, based on the polynomial recursive fitting, the vibration displacement data of the transformer under different bias magnetism are analyzed to obtain the relationship between vibration displacement and frequency, which provides a more direct prediction method for the preliminary analysis of transformer key components deformation under DC bias magnetism in engineering.
3. Finally, based on the magnetic-mechanical coupling analysis, the maximum vibration displacement occurs in the middle of the core upper clamp in the structural parts of the transformer body; and the oil tank is prone to the maximum deformation at the cover, which needs to be considered in the vibration reduction design.

## Acknowledgement

This work was supported by Shenyang Technology Bureau Fund under grant no.21-104-1-13.

## 6. Conflicts of interest

The authors declare that they have no competing interest.

## References

- [1] J. Pallot, C. Ekanayake, H. Ma, and L. Naranpanawe, (2022) "Application of operational modal analysis to investigate transformer vibration patterns" *IET Generation, Transmission & Distribution* 16(10): 1964–1973. DOI: [10.1049/gtd2.12406](https://doi.org/10.1049/gtd2.12406).
- [2] F. Zhang, S. Ji, Y. Shi, C. Zhan, and L. Zhu, (2019) "Investigation on vibration source and transmission characteristics in power transformers" *Applied Acoustics* 151: 99–112. DOI: [10.1016/j.apacoust.2019.03.011](https://doi.org/10.1016/j.apacoust.2019.03.011).

- [3] Y. Hu, J. Zheng, and H. Huang, (2019) "Experimental research on power transformer vibration distribution under different winding defect conditions" **Electronics** 8(8): 842. DOI: [10.3390/electronics8080842](https://doi.org/10.3390/electronics8080842).
- [4] P. Jiang, Z. Zhang, J. Zhang, B. Deng, J. Deng, and Z. Pan, (2022) "Research on vibration characteristics and Multi-parameter state recognition of  $\pm 500$  kV converter transformer under fluctuating conditions" **International Journal of Electrical Power & Energy Systems** 136: 107748. DOI: [10.1016/j.ijepes.2021.107748](https://doi.org/10.1016/j.ijepes.2021.107748).
- [5] X. Liu, C. Sun, Y. Wang, F. Jiang, and C. Zhang, (2021) "Vibration characteristic analysis of transformers influenced by DC bias based on vibration half-wave energy method" **International Journal of Electrical Power & Energy Systems** 128: 106725. DOI: [10.1016/j.ijepes.2020.106725](https://doi.org/10.1016/j.ijepes.2020.106725).
- [6] S. Jin. "Analysis of Vibration Characteristic of Single-Phase Three-Limb Transformer under DC Bias". In: *IOP Conference Series: Materials Science and Engineering*. 677. 5. IOP Publishing. 2019, 052060. DOI: [10.1088/1757-899X/677/5/052060](https://doi.org/10.1088/1757-899X/677/5/052060).
- [7] Z. Zhang, S. Xu, J. Zhang, H. Liu, X. Huang, Z. Wang, and L. Zhao. "Study on vibration noise signal characteristics of 10kv distribution transformer under different load conditions". In: *IOP Conference Series: Materials Science and Engineering*. 486. 1. IOP Publishing. 2019, 012033. DOI: [10.1088/1757-899X/486/1/012033](https://doi.org/10.1088/1757-899X/486/1/012033).
- [8] H. Wang, L. Zhang, Y. Sun, G. Wang, and L. Zou, (2022) "A Vibration Similarity Model of Converter Transformers and Its Verification Method" **Symmetry** 14(1): 143. DOI: [10.3390/sym14010143](https://doi.org/10.3390/sym14010143).
- [9] H. Deng, H. Shi, and Y. Qi. "Test Research on Vibration State of Transformer in High Speed EMU". In: *Journal of Physics: Conference Series*. 1678. 1. IOP Publishing. 2020, 012029. DOI: [10.1088/1742-6596/1678/1/012029](https://doi.org/10.1088/1742-6596/1678/1/012029).
- [10] Z. Zhang, Y. Wu, S. Zhang, P. Jiang, and H. Ye. "Online monitoring research of transformer vibration based on labview". In: *Journal of Physics: Conference Series*. 1168. 2. IOP Publishing. 2019, 022083. DOI: [10.1088/1742-6596/1168/2/022083](https://doi.org/10.1088/1742-6596/1168/2/022083).
- [11] X. Liu, Y. Yang, Y. Huang, and A. Jadoon, (2018) "Vibration characteristic investigation on distribution transformer influenced by DC magnetic bias based on motion transmission model" **International Journal of Electrical Power & Energy Systems** 98: 389–398. DOI: [10.1016/j.ijepes.2017.12.032](https://doi.org/10.1016/j.ijepes.2017.12.032).
- [12] X. Miao, P. Jiang, F. Pang, Y. Tang, H. Li, G. Qu, and J. Li, (2023) "Numerical analysis and experimental research of vibration and noise characteristics of oil-immersed power transformers" **Applied Acoustics** 203: 109189. DOI: [10.1016/j.apacoust.2022.109189](https://doi.org/10.1016/j.apacoust.2022.109189).